Green Chemistry

PAPER

View Article Online
View Journal | View Issue

Cite this: *Green Chem.*, 2024, **26**, 7198

An *in situ* generated proton initiated aromatic fluoroalkylation *via* electron donor–acceptor complex photoactivation†

Panyi Huang,[a] Chun Lv,[a] Haijing Song,[a] Chenjing Wang,[a] Junze Du,[a] Jianjun Li,[a,b] Bin Sun*[a,b] and Can Jin*[a,b]

Received 8th February 2024,
Accepted 10th May 2024

DOI: 10.1039/d4gc00728j

rsc.li/greenchem

The photoactivation of electron donor–acceptor complexes to obtain fluoroalkyl arenes provides an economical and environment-friendly means of directly installing fluoroalkyl groups ($-CF_2H$, $-CF_3$, $-C_4F_9$, $-C_6F_{13}$, *etc.*) in late-stage drug discovery. However, recent progress in the field has been constrained to the use of electron-rich arenes as electron donors due to their inherent electronic properties. In comparison, the role reversal strategy of using commercial fluoroalkyl reagents as donors and various aromatic substrates as acceptors remains an unexplored frontier. Herein, we proposed a photoactivation of electron donor–acceptor (EDA) complexes between fluoroalkyl sulfonates (donors) and *in situ*-generated protonated aromatic hydrocarbons (catalytic acceptors) to achieve the C–H fluoroalkylation and tandem cyclization/fluoroalkylation of more than 80 (hetero)arenes. The process relies on available reagents, avoiding the need for metals, exogenous photocatalysts, and additives.

Introduction

The distinctive effect of introducing fluorine containing groups towards lipophilicity, metabolic stability, and bioavailability enables organofluorine chemistry to play a critical role in drug development.[1] Direct C(sp^2)–H fluoroalkylation using abundant (hetero)aromatic resources can eliminate the requirement for pre-functionalization in traditional methods, thus offering atom-economical approaches.[2] The crucial advance was made by Baran and MacMillan who pioneered the direct fluoroalkylation of (hetero)arenes using conventional oxidation of fluoroalkyl precursors by peroxide and photocatalysis to generate CF_3 and CF_2H shell-opening intermediates.[3] However, a large portion of the trifluoromethyl radicals are consumed by side reactions, resulting in the use of super-stoichiometric fluoroalkyl reagents and peroxides to achieve desirable yields. To avoid harsh reaction conditions, the application of metal catalysts (Cu, Pt, Pd, Co, Ni),[4] organic dyes (rose bengal),[5] homogeneous photoconjugates of transition metals (Ru-, Ir-, and Ni-),[6] and non-homogeneous semiconductor photocatalysts (g-C_3N_4, TiO_2, CdSe)[7] has been advanced for the radical aryl C–H fluoroalkylation (Scheme 1a). These procedures eliminate the necessity for using substantial quantities of peroxide through the utilization of 5–10 mol% catalyst. However, the requirement for less abundant ruthenium- and platinum-based metals, the problem of metal residues, and the cost of catalyst procurement have stimulated the search for economical, safe, and environmentally friendly fluoroalkylation strategies.

The utilization of visible light to trigger the desired radical reactivity has transformed many traditional reaction pathways by virtue of its high efficiency and gentleness.[8] Unfortunately, both (hetero)aromatic and conventional fluoroalkyl precursors are colorless presenting absorption curves in the ultraviolet region, which cannot independently absorb low-energy photons to trigger high-energy shell-opening intermediates in the absence of external photocatalysts. To compensate for this deficiency, recent photocatalytic protocols using electron-deficient fluoroalkyl molecules (acceptors) and additional amines (sacrificial donors) or electron-rich aromatic molecules (donors) to form colored electron donor–acceptor (EDA) complexes with smaller HOMO–LUMO gaps that can absorb lower energy radiation in the visible region compared to the individual components have recently been developed (Scheme 1b).[9] Stephenson and coworkers have achieved (hetero)arene trifluoromethylation through the formation of EDA complexes between the pyridine *N*-oxide/trifluoroacetic anhydride adduct and arenes.[10] Later, the Stephenson group converted the donor from an aromatic substrate to a catalytic amount of an exogenous donor (2-methoxynaphthalene), providing opti-

[a]*College of Pharmaceutical Sciences, Collaborative Innovation Center of Yangtze River Delta Region Green Pharmaceuticals, Zhejiang University of Technology, Hangzhou 310014, China. E-mail: jincan@zjut.edu.cn, sunbin@zjut.edu.cn*
[b]*Key Laboratory for Green Pharmaceutical Technologies and Related Equipment of Ministry of Education and Key Laboratory of Pharmaceutical Engineering of Zhejiang Province, Zhejiang University of Technology, Hangzhou 310014, PR China*

† Electronic supplementary information (ESI) available. See DOI: https://doi.org/10.1039/d4gc00728j

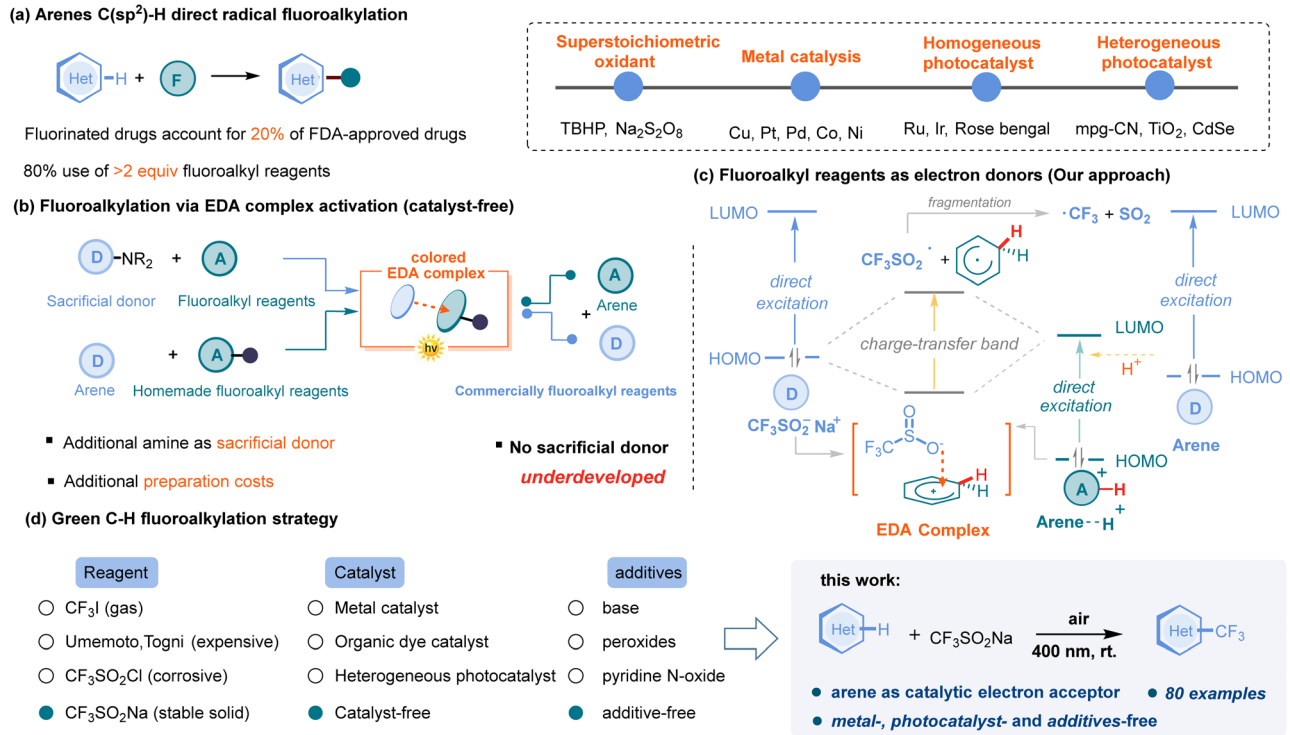

Scheme 1 Background and our working hypothesis.

mized trifluoromethylation conditions.[11] A similar EDA pathway was recently reported by the Li group who designed various perfluoroalkyl precursors containing aryl ketones as a recognition element of the EDA receptor.[12] The above EDA strategies rely on modification of fluoroalkyl precursors *via* preinstalling recognition fragments (acetylated pyridine *N*-oxide, aryl ketone, *etc.*). Neutral and electron-rich aromatic hydrocarbons have a high ionization potential, leading them to consistently act as donors.[13] If an EDA complex can be developed employing available fluoroalkyl reagents as donors and arenes as acceptors, it would enable a trifluoromethylation pathway with role reversal.

The commercial Langlois reagent (CF_3SO_2Na, an inexpensive stable solid) was considered as a potential electron-donor molecule because of the existence of an appropriate leaving group (SO_2) that can trigger irreversible cleavage events to form radical fragments at a rate competing with the back electron transfer (BET).[14] The Mulliken theory predicts that the charge transfer (CT) bands of the complexes will be redshifted with increasing electron donation or electron acceptance.[15] Therefore, a suitable reactive label needs to be sought that can enhance the electron affinity of the arenes to become acceptors. As a conceptual blueprint, the interaction of arenes (Ar) with acids to afford [Ar–H^+] adducts provided inspiration.[16] Owing to the high electron acceptance of protonated aromatics with reduced LUMO orbital energy,[17] we envisage proton adducts as catalytic acceptors to acquire EDA complexes with CF_3SO_2Na through electrostatic recognition, then S_EAr processes regenerate the protons to complete the cycle (Scheme 1c). Herein, we first propose an EDA complex between *in situ*-generated protonated aromatic hydrocarbons (catalytic acceptors) and fluoroalkyl sulfonates (donors) to achieve the fluoroalkylation of a series of (hetero)arenes. This approach avoids the need for super-stoichiometric oxidants, metals, and electron sacrificial agents, and can effectively initiate fluoroalkyl radicals through the catalytic *in situ*-generated protons (Scheme 1d).

Table 1 Optimization of the reaction conditions[a]

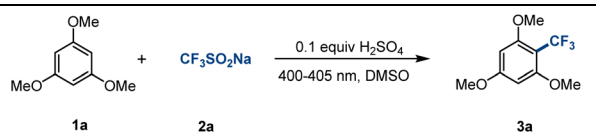

Entry	Variation from standard conditions[a]	Yield[b] of **3a** (%)
1	None	76
2	CF_3SO_3H as a proton source	79
3	HCl as a proton source	74
4	H_3PO_4 as a proton source	70
5	CH_3CO_2H as a proton source	67
6[c]	1 equiv. CF_3SO_3H as a proton source	76
7[c]	2 equiv. CF_3SO_3H as a proton source	67
8	No acid	49, 78[d]
9	In the dark	0

[a] Standard conditions: **1a** (0.3 mmol), **2a** (1.5 equiv.), acid (0.1 equiv.), DMSO (2 mL), air, rt, 5 h under 400–405 nm irradiation. [b] Isolated yield. [c] 3 h under 400–405 nm irradiation. [d] 10 h under 400–405 nm irradiation.

Results and discussion

Considering the above factors, we made a preliminary attempt to react 1,3,5-trimethoxybenzene (**1a**) with CF_3SO_2Na (**2a**) after the addition of 0.1 equiv. H_2SO_4 under 400–405 nm irradiation, and the desired CF_3-substituted product **3a** was obtained in 76% yield (Table 1, entry 1). Encouraged by this result, a variety of acids were investigated for this transformation process (Table 1, entries 2–5). The experiment showed that CF_3SO_3H (pK_a = 0.3 in DSMO) promoted the reaction best and CH_3COOH (pK_a = 12.6 in DMSO) worst with the same irradiation time, which was positively correlated with the ability of the acid to provide protons. When adding 2 equiv. CF_3SO_3H, the reaction rate is decreased as compared to 1 equiv. CF_3SO_3H (Table 1, entries 6 and 7), which may be due to the reduction of concentration of free aromatic hydrocarbons in the system. Surprisingly, the target product **3a** was obtained in 78% yield by prolonging the reaction time without the addition of a Brønsted acid (Table 1, entry 8). The pH value, high-resolution mass spectrometry, and ^{19}F NMR showed that **2a** was transformed into CF_3SO_3H at a slow rate under continuous 400–405 nm irradiation in air, which leads to *in situ* generation of protons (see the ESI, Fig. S2–4, for details†). Considering the cost of the reagents and the environmental impact, entry 8 sacrificing some of the reaction rate but representing greener conditions, was determined to be the optimal conditions. The control experiments suggested that light was necessary for this transformation (Table 1, entry 9).

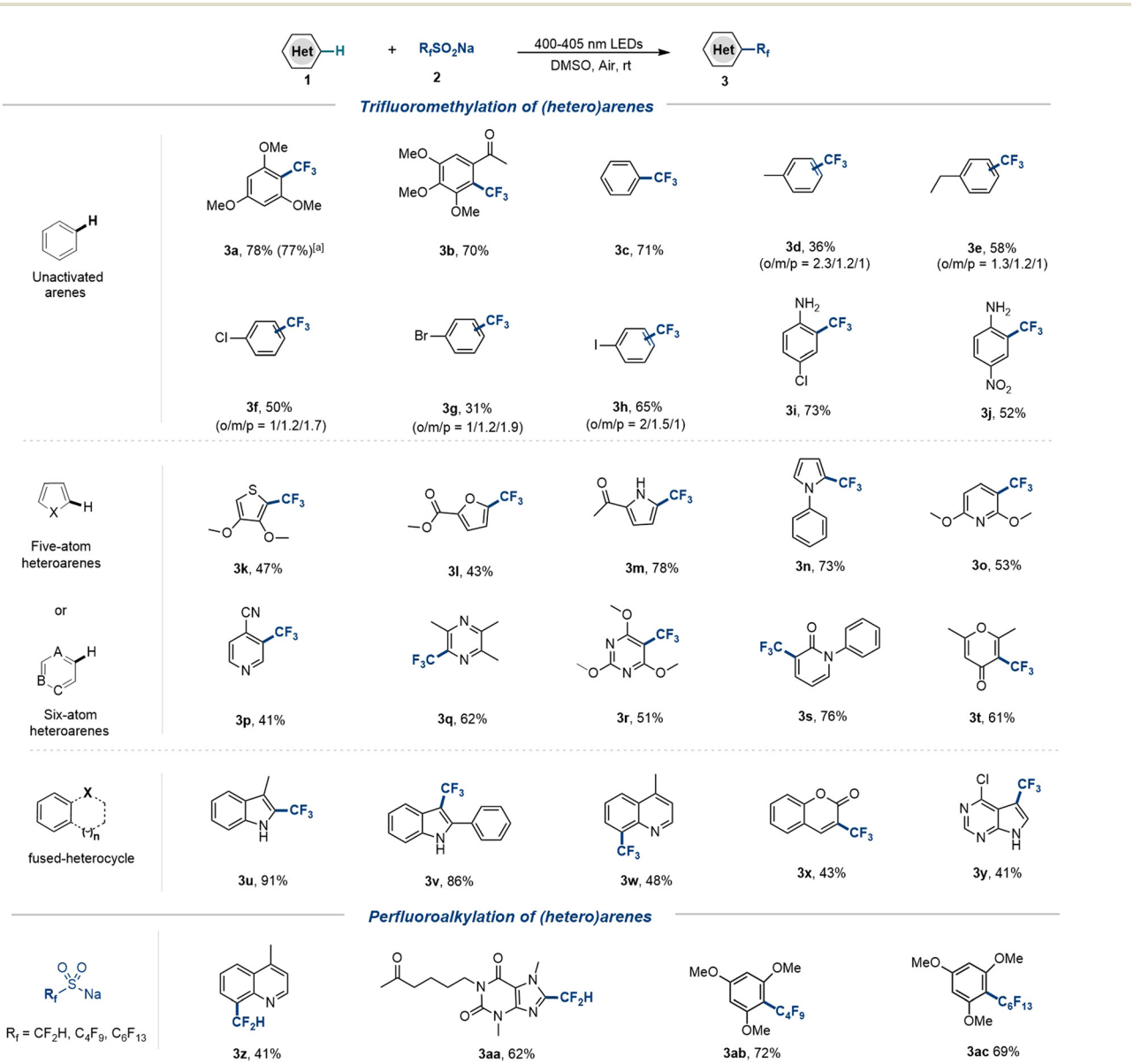

Scheme 2 Substrate scope of aromatic fluoroalkylation. Reaction conditions: **1** (0.30 mmol, 1.0 equiv.), **2** (0.45 mmol, 1.5 equiv.), DMSO (2.0 mL), 6–32 h, under 400–405 nm irradiation in air. [a]Gram-scale.

In order to further assess the scope of the protocol, C–H trifluoromethylation of other (hetero)arenes was investigated under the optimized conditions (Scheme 2). Electron-rich and neutral arenes were converted to valuable trifluoromethylated derivatives in high yields (**3a–3c**). Notably, alkyl aromatics, halohydrocarbons, and arylamines that are not tolerated with many reaction conditions (such as oxidants, transition metals, chemically equivalent acids, and ultraviolet light) can yield chemicals needed for industrial production (**3d–3i**). In addition, the electron-withdrawing groups NO_2 and CN are tolerated although in a lower yield (**3j**, **3p**). Thiophene, furan, pyrrole, pyridine, pyrazine, pyrimidine, pyridone, pyrone, and other five- and six-membered heterocycles as drug pharmacophores are compatible with the trifluoromethylation strategy (**3k–3t**). The indoles, quinoline, coumarin, and 7-diazapurine with various potential reaction sites displayed high regioselectivity for C–H trifluoromethylation at the most electron-rich positions (**3u–3y**). In addition, the application of other

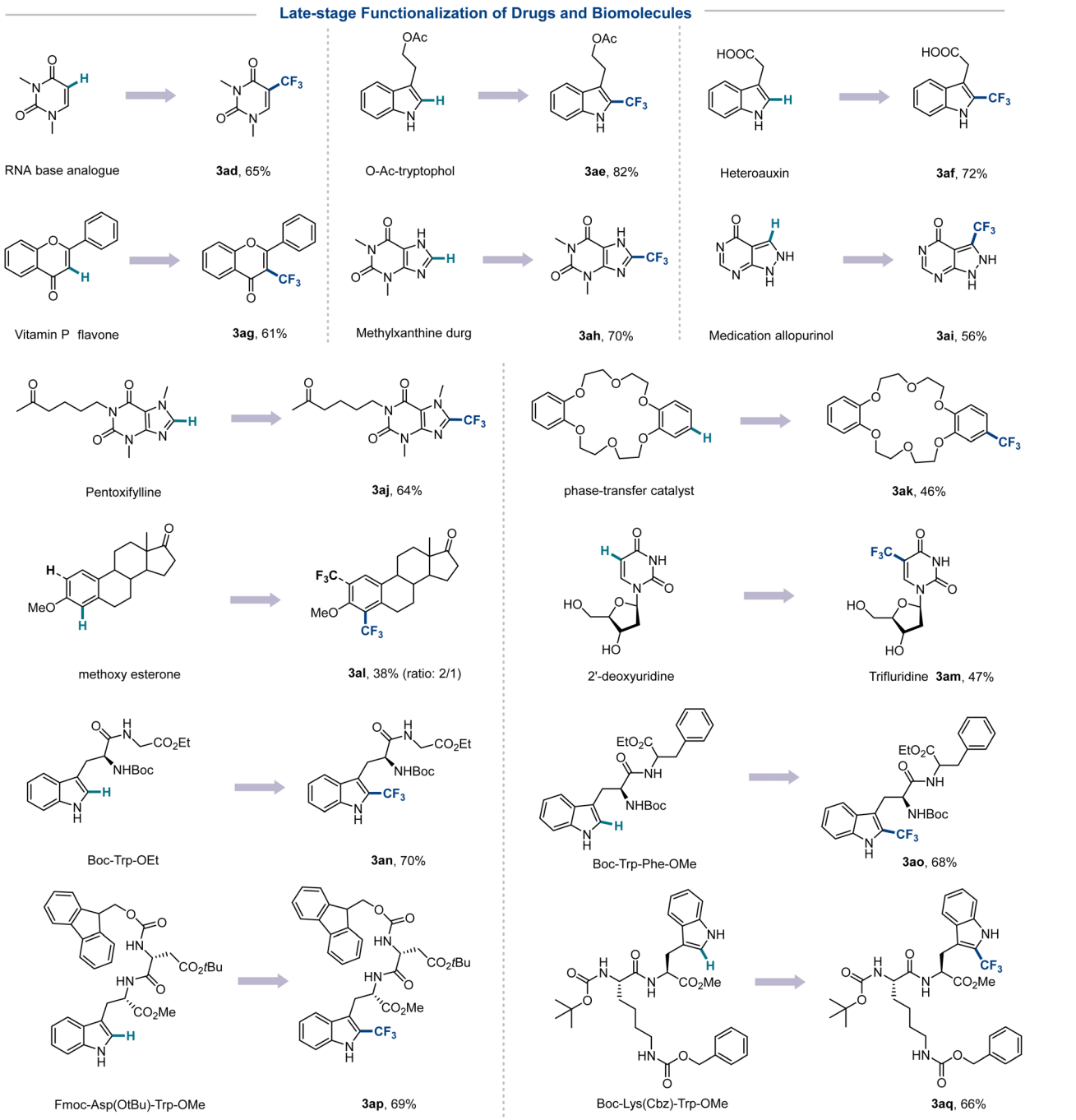

Scheme 3 Trifluoroalkylation of drugs and biomolecules. Reaction conditions: **1** (0.30 mmol, 1.0 equiv.), **2** (0.45 mmol, 1.5 equiv.), DMSO (2.0 mL), 6–24 h, under 400–405 nm irradiation in air.

fluoroalkyl sulfonates to 1,3,5-trimethoxybenzene, quinoline and pentoxifylline was successful in the incorporation of perfluoroalkyl and CF_2H groups that commonly act as bioequivalents of hydroxyls and amides (**3z–3ac**). Gratifyingly, several drugs, bioactive molecules, and hormones, including dimethyluracil **1ad** (RNA base analogue), tryptophol **1ae** (metabolite), heteroauxin **1af** (endogenous phytohormone), flavone **1ag** (vitamin P), theophylline **1ah** (respiratory drug), allopurinol **1ai** (uric acid lowering drug), pentoxifylline **1aj** (PDE inhibitor), dibenzo-18-crown-6 **1ak** (phase-transfer catalyst), and estrone **1al** (steroid hormone) are capable of late-stage functionalization through a simple trifluoromethylation strategy (Scheme 3). In addition, the antiviral drug trifluridine **3am** can be prepared in one step by simply mixing 2′-deoxyuridine **1am** with CF_3SO_2Na without adding any additives needed in the conventional production process. The structurally complex peptides in the presence of Gly (**1an**), Phe (**1ao**), Asp (**1ap**), and Lys (**1aq**) units afforded trifluoromethylated peptides at the C2 position of the Trp residue with retention of chirality, providing a mild and efficient tool for late-stage modifications in protein engineering.

Besides arene C(sp^2)–H direct radical fluoroalkylation, we sought to extend the strategy to C(sp^2)–H fluoroalkylation/tandem cyclization for accessing fluoroalkyl-substituted polycyclic backbones with pharmaceutical potential (Scheme 4).[18] The study was initiated with benzimidazoles containing unactivated alkenes without further optimization of the previously determined reaction conditions (**5a**). Regardless of electronic bias, substituted benzimidazoles, containing methyl, ester, halogen, cyano, and trifluoromethyl substituents on the

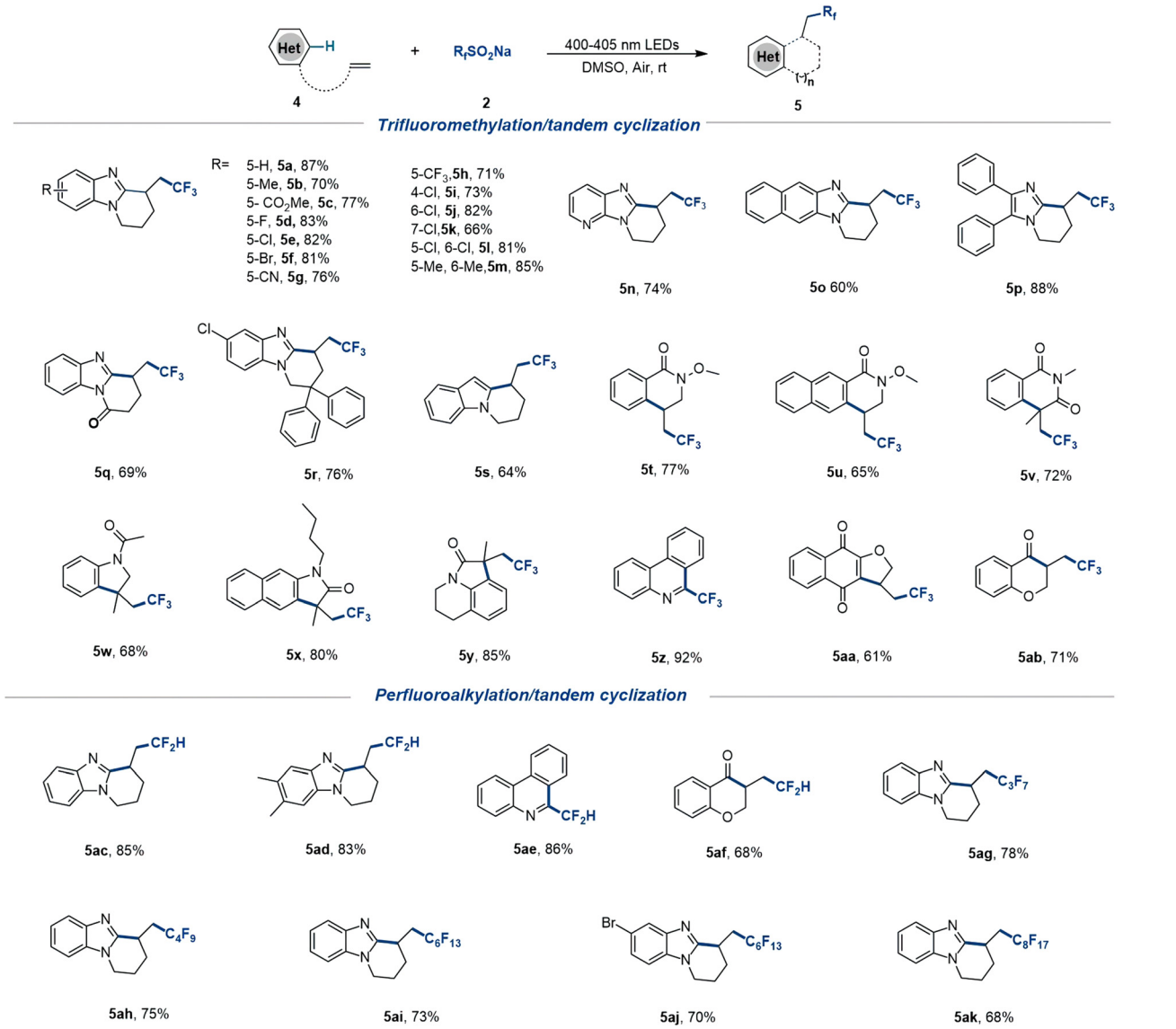

Scheme 4 Substrate scope of fluoroalkylation/cyclization. **4** (0.30 mmol, 1.0 equiv.), **2** (0.45 mmol, 1.5 equiv.), DMSO (2.0 mL), 12 h, under 400–405 nm irradiation in air.

benzene ring, can be employed to access the polycyclic benzimidazoles **5b–5h** in 70%–83% yield. Benzimidazoles disubstituted and monosubstituted at different positions can be smoothly transformed into the corresponding products (**5i–5m**). Moreover, pyridine, naphthalene, imidazole skeletons, and diverse branched olefins are adaptable to the current strategy (**5n–5r**). Inspiringly, the mild tandem cyclization strategy is also applicable to the synthesis of trifluoromethylated polycyclic indoles, dihydroisoquinolones, isoquinolinones, indolines, tricyclic oxindoles, phenanthridines, polycyclic 1,4-naphthoquinones, and chromanones (**5s–5ab**). Finally, C(sp^2)–H perfluoroalkylation cyclization provides the target products **5ac–5ak** in 68%–86% yield.

To explore the mechanism of aromatic trifluoromethylation, we have performed control experiments as shown in Scheme 5 and the ESI.† Firstly, the transformation was completely restrained upon the addition of TEMPO or 1,1-diphenylethylene radical scavengers under the standard conditions, and the captured intermediates were detected by ESI-MS or ^{19}F NMR, which indicated the formation of trifluoromethyl radicals (Scheme 5a). When the template reaction was performed with CF_3SO_2Na which was irradiated for 48 h the desired product could not be obtained. However, if the proportion of CF_3SO_2Na pre-irradiated was decreased to 6%, the reaction could proceed smoothly to deliver **3a** in 80% yield in 6 h, which is consistent with the conclusion that CF_3SO_3H is formed from **2a** when irradiated in air. Subsequently, the desired product **3a** was not observed when the template reaction was irradiated under a nitrogen atmosphere. However, the standard protocol gave **3a** in 47% yield under a nitrogen atmosphere with the addition of 1 equiv. CF_3SO_3H. These findings support the key role of oxygen in promoting the *in situ* for-

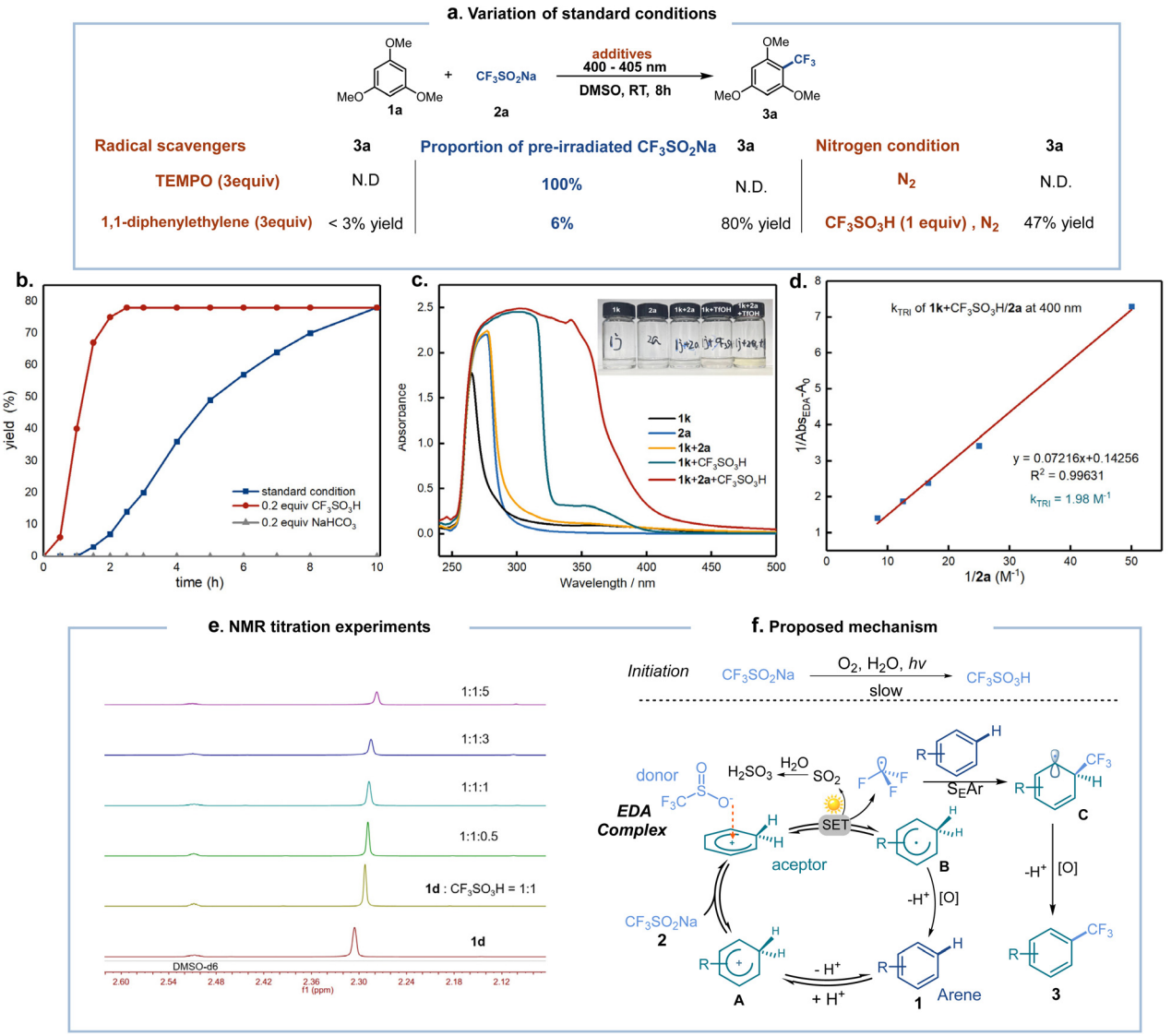

Scheme 5 Mechanistic studies. (a) Variation of standard conditions. (b) Monitoring of reaction processes. (c) UV/vis absorption spectra. (d) Benesi–Hildebrand plot. (e) NMR titration experiments. (f) Proposed mechanism.

mation of protons from **2a**. Next, adding CF_3SO_3H showed a faster rate mainly due to eliminating the induction period for the *in situ* formation of protonated aromatics. In contrast, the addition of $NaHCO_3$ strongly inhibited the reaction, and no product was provided even after extending the reaction time to 24 h (Scheme 5b). To clarify the effect of protons in the process, the individual and mixed fractions were analyzed by UV/vis absorption spectroscopy (Scheme 5c). The thiophene (**1k**) or CF_3SO_3Na (**2a**) only displayed absorption curves in the UV region, while the redshift of the mixed solution of **1k** and CF_3SO_3H demonstrates the possible formation of protonated aromatic hydrocarbons (green line). The absorption band tail of the mixture of **1k**, **2a**, and CF_3SO_3H extends to the visible region (red line) compared with the mixture of **1k** and **2a** (yellow line), indicating that the acid promotes the formation of an EDA complex between the aromatic hydrocarbons and the fluoroalkyl sulfonate. The same phenomenon was obtained by performing UV/visible absorption experiments on benzene (**1c**) (for details, see the ESI, Fig. S9†). Moreover, the existence of the EDA complex was also verified using Benesi–Hildebrand experiments with an association constant of 1.98 M^{-1} in DMSO (Scheme 5d). NMR titration experiments were carried out and the ^1H NMR signal was gradually shifted downfield as **2a** was increased in the presence of CF_3SO_3H and toluene (**1d**) in a 1 : 1 ratio (Scheme 5e). The quantum yield (Φ = 0.14) determined by chemical actinometry and on/off experiments preclude a chain radical mechanism, as shown in Fig. S16.† Overall, these studies revealed the presence of protonated aromatic hydrocarbons generated *in situ* and that they play a crucial role in the formation of EDA complexes.

Based on the above experiments, a proposed mechanism is depicted in Scheme 5f. The reaction is initiated by the formation of CF_3SO_3H with **2a** and H_2O under 400–405 nm light irradiation. Aromatic hydrocarbons then undergo protonation to form EDA complexes with **2a**. The charge transfer event within the complex leads to the generation of trifluoromethyl radicals with the release of sulfur dioxide under 400–405 nm irradiation. In the presence of free aromatic hydrocarbons, the former trifluoromethyl radical can be efficiently captured to create a radical electrophilic adduct **C**. Subsequently, the oxidation and deprotonation of the adducts provides the trifluoromethyl-substituted arene and regenerates the proton to activate another aromatic substrate.

Conclusions

In conclusion, EDA complexes of *in situ-generated* protonated aromatic hydrocarbons with fluoroalkyl sulfonates are proposed to achieve C–H fluoroalkylation and tandem cyclization/fluoroalkylation of heteroaromatic hydrocarbons. Differing from the previous approach of aromatics as donors and fluoroalkyl reagents as acceptors, a simple activation program enabled a strategy for role reversal. This versatile activation mode of EDA complexes was presented for the first time. Various (hetero)arenes are used to construct fluorinated motifs in a green and efficient way without exogenous photocatalysts and additives. The practicability of this protocol is also emphasized by the late-stage functionalization of bioactive molecules.

Conflicts of interest

There are no conflicts to declare.

Acknowledgements

This work was supported by the National Natural Science Foundation of China (Grant No. 22078299 and 22108250) and Zhejiang Provincial Natural Science Foundation of China (LY21B060005, LQ20B060007). We are also grateful to the College of Pharmaceutical Sciences, Zhejiang University of Technology and Collaborative Innovation Center of Yangtze River Delta Region Green Pharmaceuticals for the financial help.

References

1 (*a*) C. Alonso, E. M. D. Marigorta, G. Rubiales and F. Palacios, *Chem. Rev.*, 2015, **115**, 1847; (*b*) C. Le, T. Q. Chen, T. Liang, P. Zhang and D. W. C. MacMillan, *Science*, 2019, **360**, 1010; (*c*) F. Ye, F. Berger, H. Jia, J. Ford, A. Wortman, J. Bçrgel, C. Genicot and T. Ritter, *Angew., Chem. Int. Ed.*, 2019, **58**, 14615; (*d*) W.-Q. Hu, S. Pan, X.-H. Xu, D. A. Vicic and F.-L. Qing, *Angew. Chem., Int. Ed.*, 2020, **59**, 16076; (*e*) J. Yang, S. Zhu, F. Wang, F.-L. Qing and L. Chu, *Angew. Chem., Int. Ed.*, 2021, **60**, 4300; (*f*) Z.-J. Shen, C. Zhu, X. Zhang, C. Yang, M. Rueping, L. Guo and W. Xia, *Angew. Chem., Int. Ed.*, 2023, DOI: **10.1002/ange.202217244**.

2 (*a*) A. G. O'Brien, A. Maruyama, Y. Inokuma, M. Fujita, P. S. Baran and D. G. Blackmond, *Angew. Chem., Int. Ed.*, 2014, **53**, 11868; (*b*) Y. Pang, J. W. Lee, K. Kubota and H. Ito, *Angew. Chem., Int. Ed.*, 2020, **59**, 22570; (*c*) H. Jia, A. P. Häring, F. Berger, L. Zhang and T. Ritter, *J. Am. Chem. Soc.*, 2021, **143**, 7623; (*d*) H. Xiao, Z. Zhang, Y. Fang, L. Zhu and C. Li, *Chem. Soc. Rev.*, 2021, **50**, 6308; (*e*) J. Shen, J. Xu, L. He, C. Liang and W. Li, *Chin. Chem. Lett.*, 2022, **33**, 1227.

3 (*a*) Y. Fujiwara, J. A. Dixon, F. O'Hara, E. D. Funder, D. D. Dixon, R. A. Rodriguez, R. D. Baxter, B. Herlé, N. Sach, M. R. Collins, Y. Ishihara and P. S. Baran, *Nature*, 2012, **492**, 95; (*b*) Y. Fujiwara, J. A. Dixon, R. A. Rodriguez, R. D. Baxter, D. D. Dixon, M. R. Collins, D. G. Blackmond and P. S. Baran, *J. Am. Chem. Soc.*, 2012, **134**, 1494; (*c*) D. A. Nagib and D. W. C. MacMillan, *Nature*, 2011, **480**, 224–227.

4 (*a*) K. Natte, R. V. Jagadeesh, L. He, J. Rabeah, J. Chen, C. Taeschler, S. Ellinger, F. Zaragoza, H. Neumann, A. Brȕckner and M. Beller, *Angew. Chem., Int. Ed.*, 2016, **55**, 2782; (*b*) S. Deolka, R. Govindarajan, E. Khaskin, R. R. Fayzullin, M. C. Roy and J. R. Khusnutdinova, *Angew. Chem., Int. Ed.*, 2021, **60**, 24620; (*c*) H.-R. Zhang, C.-C. Feng,

N. Chen and S.-L. Zhang, *Angew. Chem., Int. Ed.*, 2023, DOI: 10.1002/ange.202209029; (*d*) S. Deolka, R. Govindarajan, T. Gridneva, M. C. Roy, S. Vasylevskyi, P. K. Vardhanapu, J. R. Khusnutdinova and E. Khaskin, *ACS Catal.*, 2023, **13**, 13127; (*e*) C. S. Kuehner, A. G. Hill, C. F. Harris, C. A. Owens, J. Bacsa and J. D. Soper, *ACS Catal.*, 2023, **13**, 13607.

5 (*a*) L. Cui, Y. Matusaki, N. Tada, T. Miura, B. Uno and A. Itoh, *Adv. Synth. Catal.*, 2013, **355**, 2203; (*b*) S. P. Pitre, C. D. McTiernan, H. Ismaili and J. C. Scaiano, *ACS Catal.*, 2014, **4**, 2530; (*c*) W. Zhang, X.-X. Xiang, J. Chen, C. Yang, Y.-L. Pan, J.-P. Cheng, Q. Meng and X. Li, *Nat. Commun.*, 2020, **11**, 638.

6 (*a*) J. W. Beatty, J. J. Douglas, K. P. Cole and C. R. J. Stephenson, *Nat. Commun.*, 2015, **6**, 7919; (*b*) B. Yang, D. Yu, X.-H. Xu and F.-L. Qing, *ACS Catal.*, 2018, **8**, 2839; (*c*) L. Trump, A. Lemos, B. Lallemand, P. Pasau, J. Mercier, C. Lemaire, A. Luxen and C. Genicot, *Angew. Chem., Int. Ed.*, 2019, **58**, 13149.

7 (*a*) J. Lin, Z. Li, J. Kan, S. Huang, W. Su and Y. Li, *Nat. Commun.*, 2017, **8**, 14353; (*b*) I. Ghosh, J. Khamrai, A. Savateev, N. Shlapakov, M. Antonietti and B. König, *Science*, 2019, **365**, 360; (*c*) K. Muralirajan, R. Kancherla, J. A. Bau, M. R. Taksande, M. Qureshi, K. Takanabe and M. Rueping, *ACS Catal.*, 2021, **11**, 14772.

8 (*a*) Y. Zhao and W. Xia, *Chem. Soc. Rev.*, 2018, **47**, 2591; (*b*) M. Latrache and N. Hoffmann, *Chem. Soc. Rev.*, 2021, **50**, 7418; (*c*) A. R. Allen, E. A. Noten and C. R. J. Stephenson, *Chem. Rev.*, 2022, **122**, 2695; (*d*) L. Chang, Q. An, L. Duan, K. Feng and Z. Zuo, *Chem. Rev.*, 2022, **122**, 2429; (*e*) A. Y. Chan, B. Perry, N. B. Bissonnette, B. F. Buksh, G. A. Edwards, L. I. Frye, O. L. Garry, M. N. Lavagnino, B. X. Li, Y. Liang, E. Mao, A. Millet, J. V. Oakley, N. L. Reed, H. A. Sakai, C. P. Seath and D. W. C. MacMillan, *Chem. Rev.*, 2022, **122**, 1485.

9 (*a*) R. Wang, W. Guan, Z.-B. Han, F. Liang, T. Suga, X. Bi and H. Nishide, *Org. Lett.*, 2017, **19**, 2358; (*b*) R. Wang, L. Wang, Q. Xu, B.-Y. Ren and F. Liang, *Org. Lett.*, 2019, **21**, 3072; (*c*) X. Liang, Y. Li, Q. Xia, L. Cheng, J. Guo, P. Zhang, W. Zhang and Q. Wang, *Green Chem.*, 2021, **23**, 8865; (*d*) A. Dewanji, L. Dalsen, J. A. Rossi-Ashton, E. Gasson, G. E. M. Crisenza and D. J. Procter, *Nat. Chem.*, 2023, **15**, 43; (*e*) H. Wang, J. Wu, A. Noble and V. K. Aggarwal, *Angew. Chem., Int. Ed.*, 2022, DOI: 10.1002/ange.202202061; (*f*) L. Dalsen, E. Brown, J. A. Rossi-Ashton and D. J. Procter, *Angew. Chem., Int. Ed.*, 2023, DOI: 10.1002/anie.202303104; (*g*) A. K. Wortman and C. R. J. Stephenson, *Chem*, 2023, **9**, 1.

10 J. W. Beatty, J. J. Douglas, R. Miller, R. C. McAtee, K. P. Cole and C. R. J. Stephenson, *Chem*, 2016, **1**, 456.

11 E. J. McClain, T. M. Monos, M. Mori, J. W. Beatty and C. R. J. Stephenson, *ACS Catal.*, 2020, **10**, 12636.

12 D. J. Castillo-Pazos, J. D. Lasso, E. Hamzehpoor, J. Ramos-Sánchez, J. M. Salgado, G. Cosa, D. F. Perepichka and C.-J. Li, *Chem. Sci.*, 2023, **14**, 3470.

13 (*a*) G. E. M. Crisenza, D. Mazzarella and P. Melchiorre, *J. Am. Chem. Soc.*, 2020, **142**, 5461; (*b*) M. R. Lasky, T. K. Salvador, S. Mukhopadhyay, M. S. Remy, T. P. Vaid and M. S. Sanford, *Angew. Chem., Int. Ed.*, 2022, DOI: 10.1002/anie.202208741.

14 (*a*) Q.-Y. Meng, N. Dçben and A. Studer, *Angew. Chem., Int. Ed.*, 2020, **59**, 19956; (*b*) Y. Jiang, B. Li, N. Ma, S. Shu, Y. Chen, S. Yang, Z. Huang, D. Shi and Y. Zha, *Angew. Chem., Int. Ed.*, 2021, **60**, 19030.

15 R. S. Mulliken, *J. Am. Chem. Soc.*, 1952, **74**, 811.

16 (*a*) Z. Huang, M. Shanmugam, Z. Liu, A. Brookfield, E. L. Bennett, R. Guan, D. E. V. Herrera, J. A. Lopez-Sanchez, A. G. Slater, E. J. L. McInnes, X. Qi and J. Xiao, *J. Am. Chem. Soc.*, 2022, **144**, 6532; (*b*) J. Wu, J. Chen, L. Wang, H. Zhu, R. Liu, G. Song, C. Feng and Y. Li, *Green Chem.*, 2023, **25**, 940.

17 W. Liu, X. Yang, Z.-Z. Zhou and C.-J. Li, *Chem*, 2017, **2**, 688.

18 (*a*) J. Xuan and A. Studer, *Chem. Soc. Rev.*, 2017, **46**, 4329; (*b*) Y. Yuan, Y. Zheng, B. Xu, J. Liao, F. Bu, S. Wang, J.-G. Hu and A. Lei, *ACS Catal.*, 2020, **10**, 6676; (*c*) S. Zheng, Á. Gutiérrez-Bonet and G. A. Molander, *Chem*, 2019, **5**, 339; (*d*) Q.-W. Gui, F. Teng, P. Yu, Y.-F. Wu, Z.-B. Nong, L.-X. Yang, X. Chen, T.-B. Yang and W.-M. He, *Chin. J. Catal.*, 2023, **44**, 111.